Georges Lemaître Center for Earth and Climate Research
(Institut d'Astronomie et de Géophysique G. Lemaître)
Chemin du Cyclotron, 2
1348 Louvain-la-Neuve

Que nous apprend le passé du climat sur son avenir ?

A. Berger et Q.Z. Yin

Cercle Gaulois artistique et littéraire, Aménagement urbain, Villes et Société
Bruxelles, 18 mars 2013

ERC Advanced Grant EMIS 2008-2013

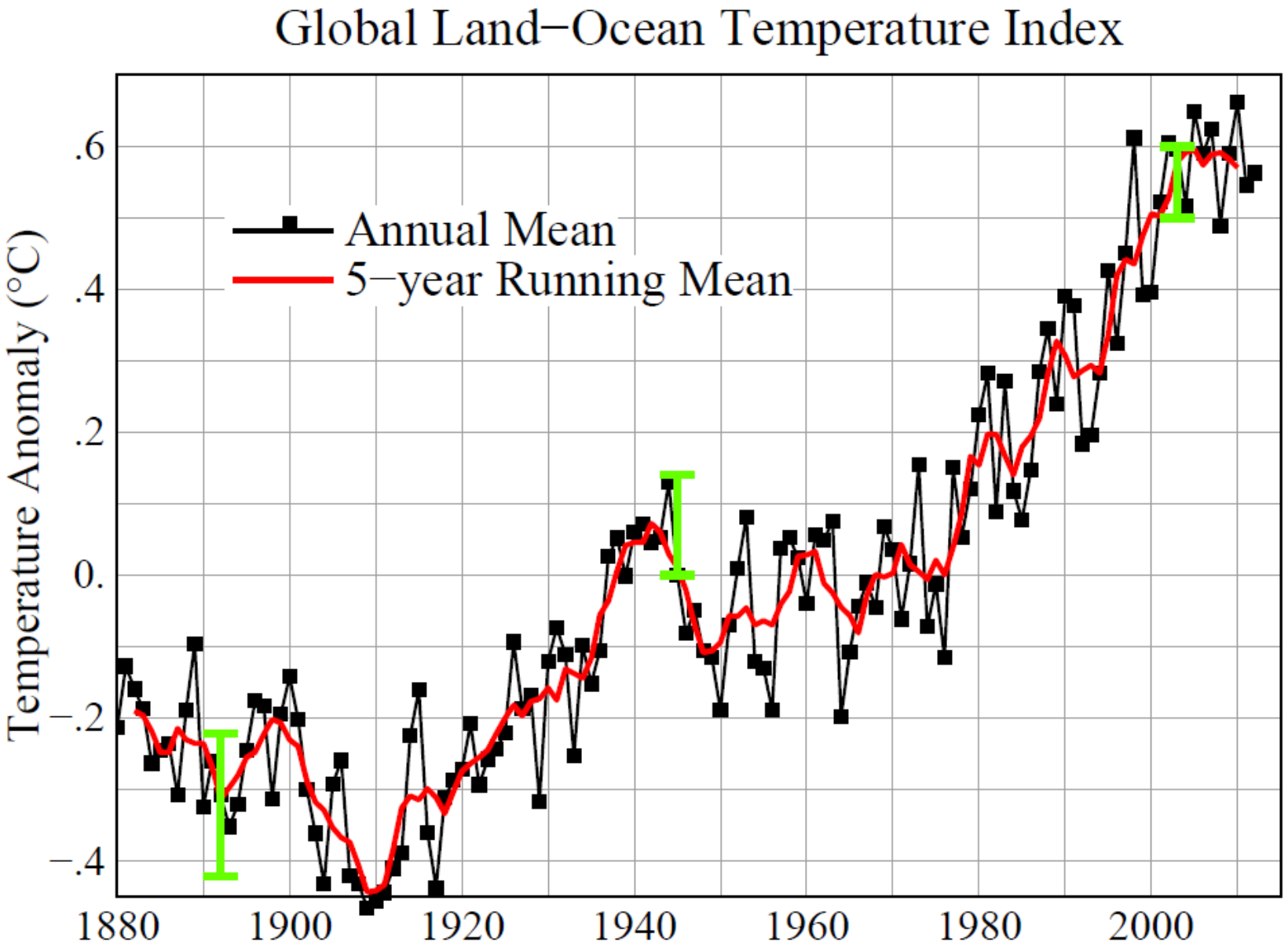

Hansen, J., Mki. Sato, R. Ruedy, K. Lo, D.W. Lea, and M. Medina-Elizade, 2006: Global temperature change. *Proc. Natl. Acad. Sci.*, **103**, 14288-14293, doi:10.1073/pnas.0606291103 http://data.giss.nasa.gov/gistemp/

1864 lithogravure

glacier d'Argentière

1896 photo

1995 Berger

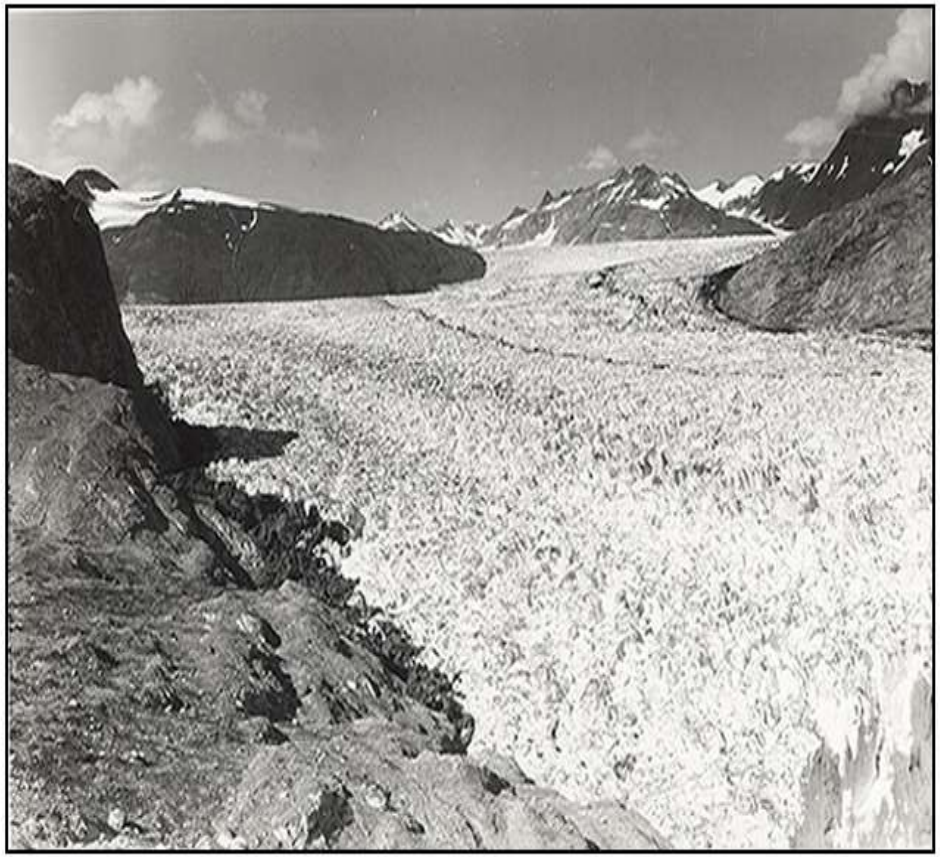

On the left is a photograph of Muir Glacier (Alaska) taken on August 13, 1941, by glaciologist William O. Field; on the right, a photograph taken from the same vantage on August 31, 2004, by geologist Bruce F. Molnia of the United States Geological Survey (USGS).

According to Molnia, between 1941 and 2004 the glacier retreated more than twelve kilometers (seven miles) and thinned by more than 800 meters.

Gravity Satellite Ice Sheet Mass Measurements

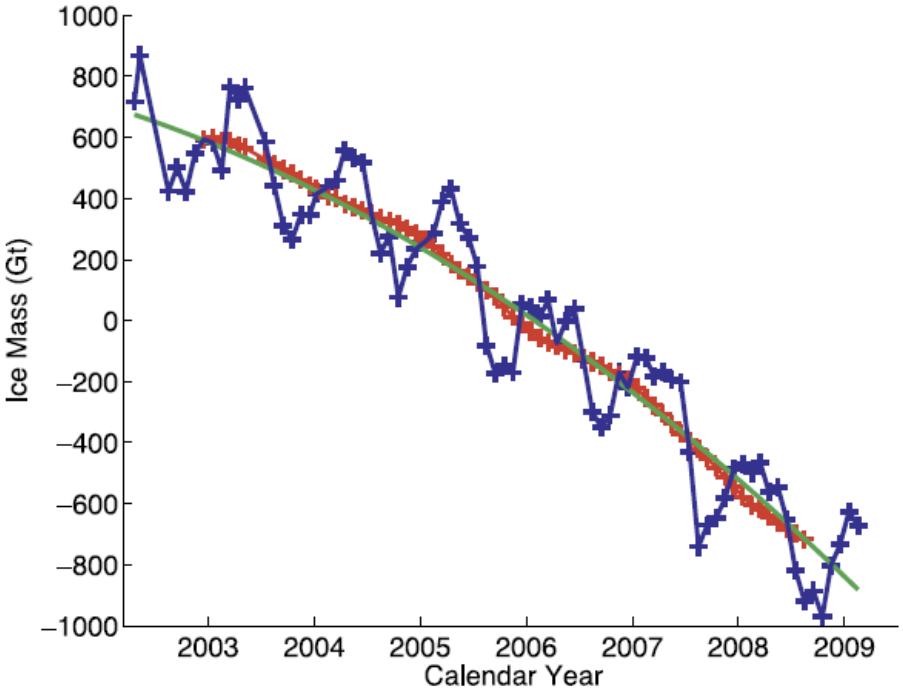

Greenland Ice Sheet

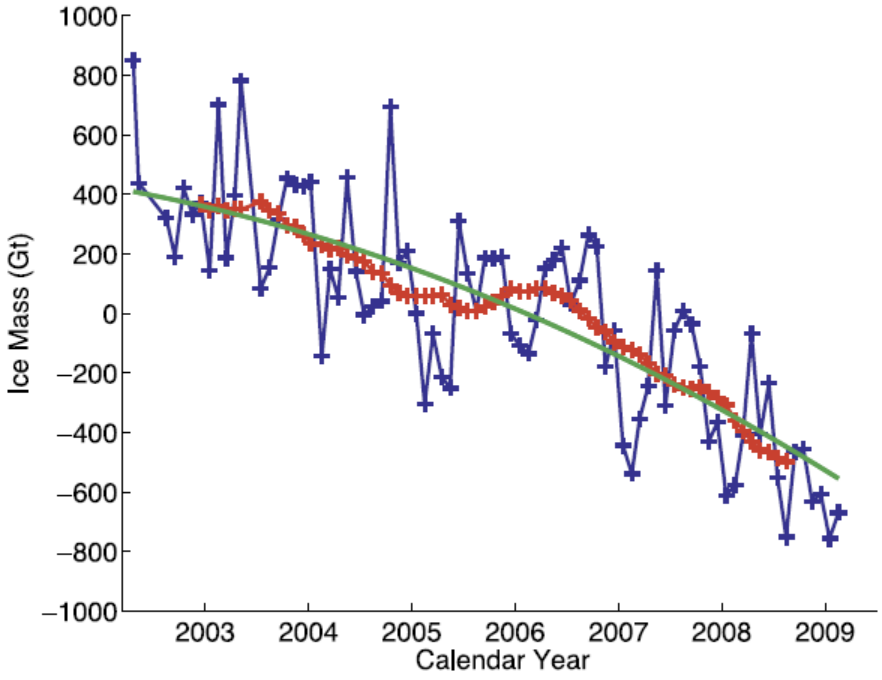

Antarctic Ice Sheet

Source: Velicogna, I. *Geophys. Res. Lett.*, **36**, L19503, doi:10.1029/2009GL040222, 2009.

Sea Level Rise

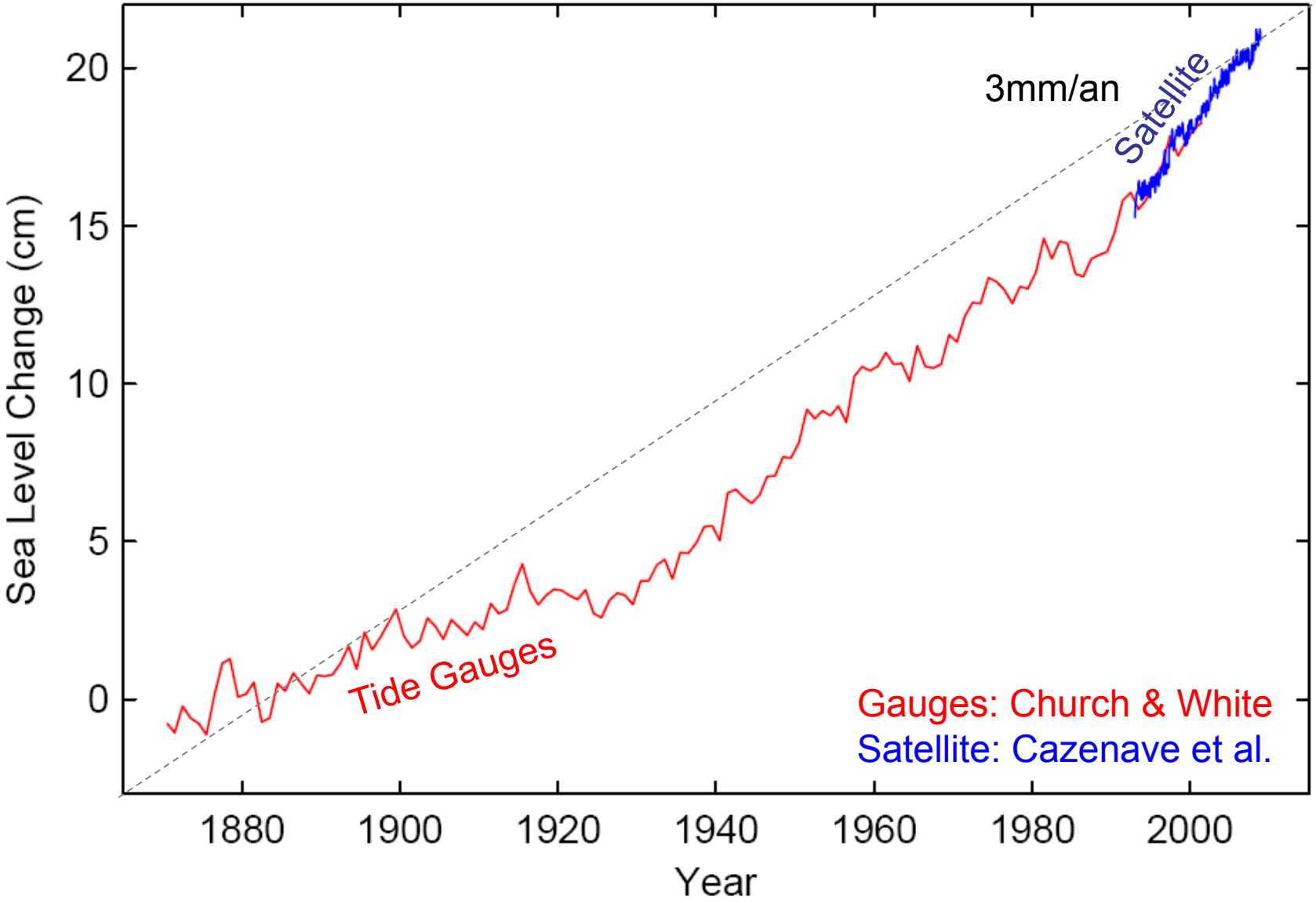

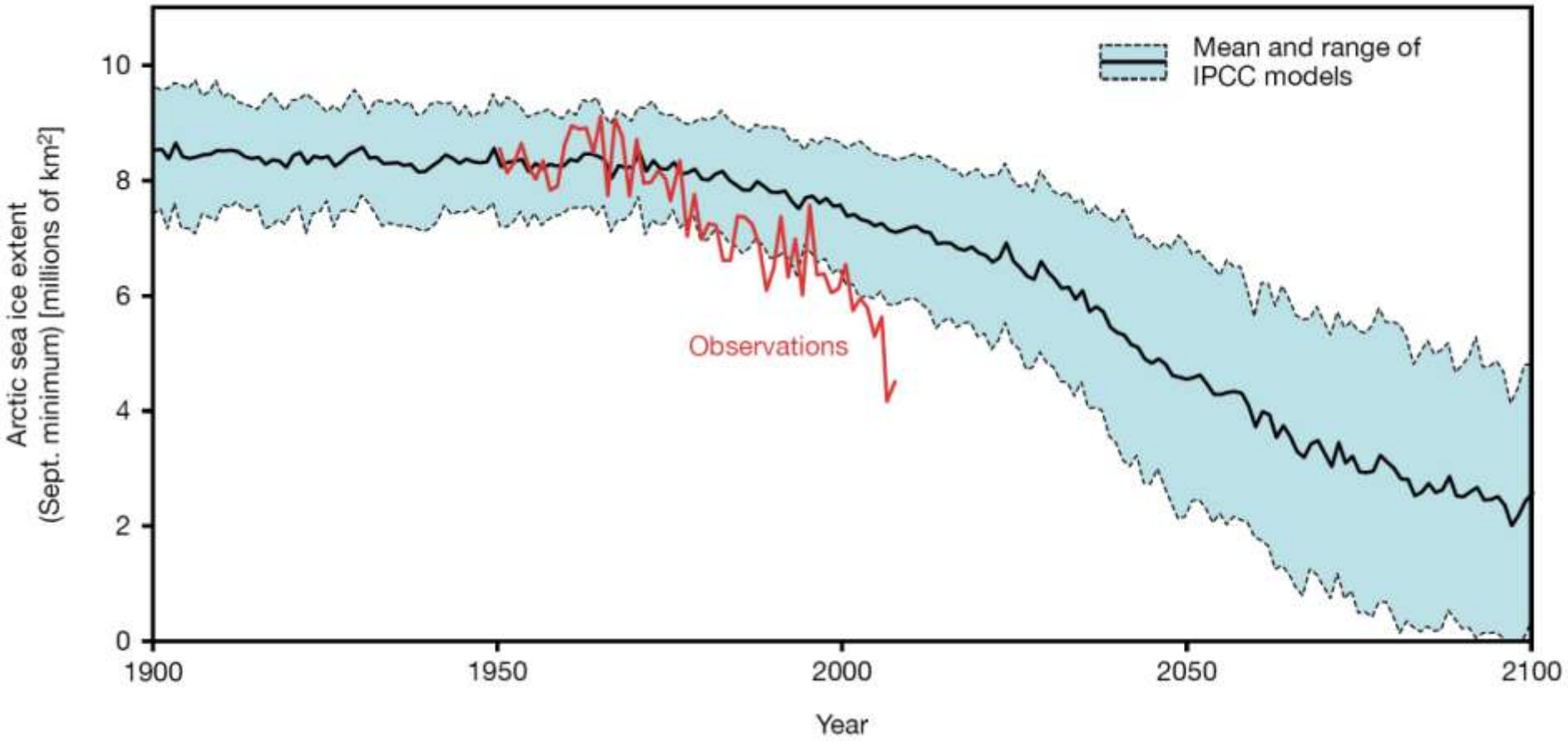

Figure 13: Observed and modeled Arctic sea-ice extent

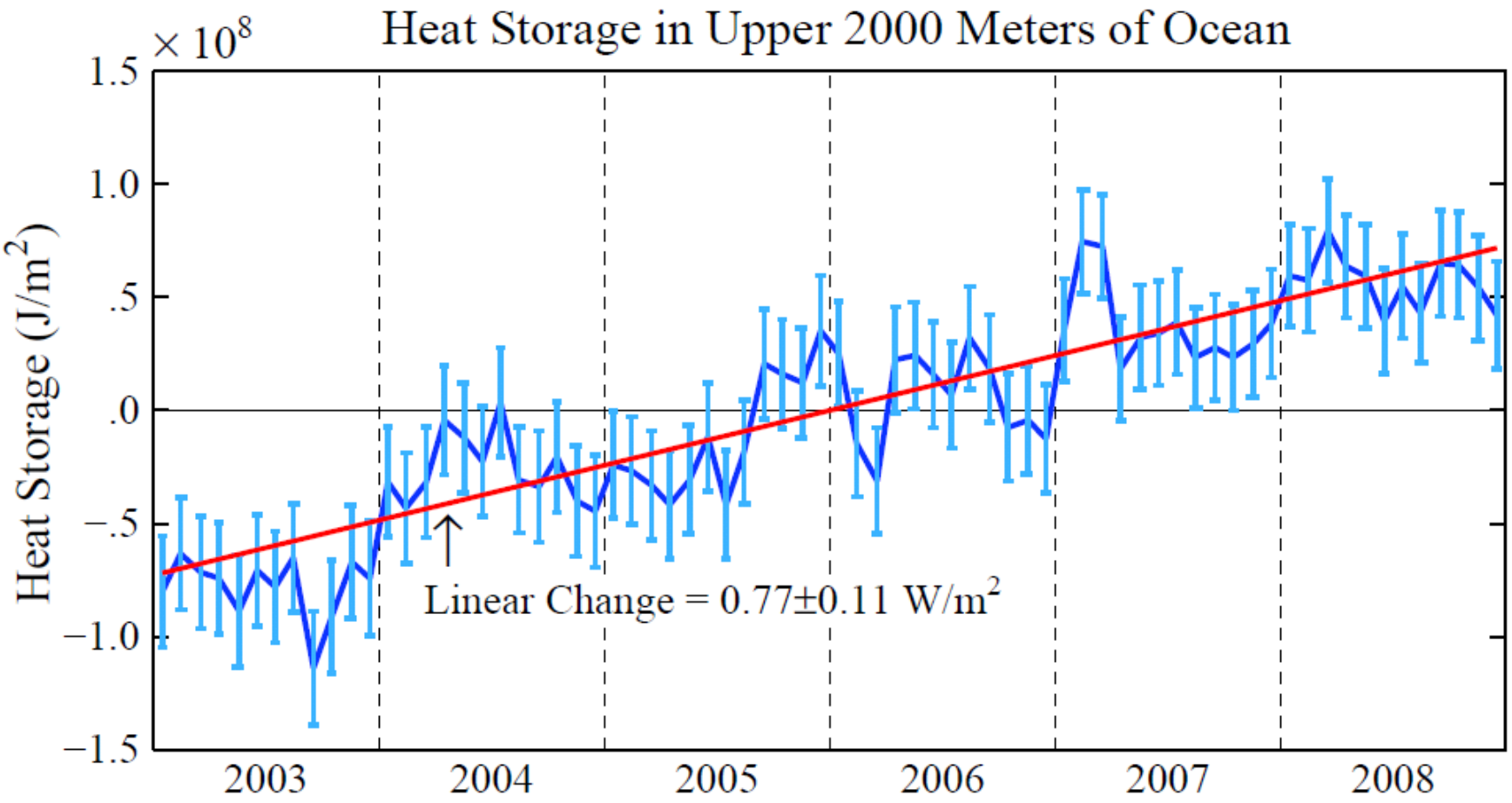

Heat storage in upper 2000 meters of ocean during 2003-2008 based on ARGO data.

Knowledge of Earth's energy imbalance is improving rapidly as ARGO data lengthens.

Data must be averaged over a decade because of El Nino/La Nina and solar variability.

Energy imbalance is smoking gun for human-made increasing greenhouse effect.

Data source: von Schuckmann *et al. J. Geophys. Res.* **114**, C09007, 2009, doi:10.1029/2008JC005237.

Changements écologiques : avancement du cycle végétatif

Date de début des vendanges à Châteauneuf-du-pape de 1945 à 2005

11-oct
6-oct
1-oct
26-sep
21-sep
16-sep
11-sep
6-sep
1-sep
27-aoû

1945 1950 1955 1960 1965 1970 1975 1980 1985 1990 1995 2000 2005

Années A.D.

Source: Service technique Inter-Rhône; base PhénoClim

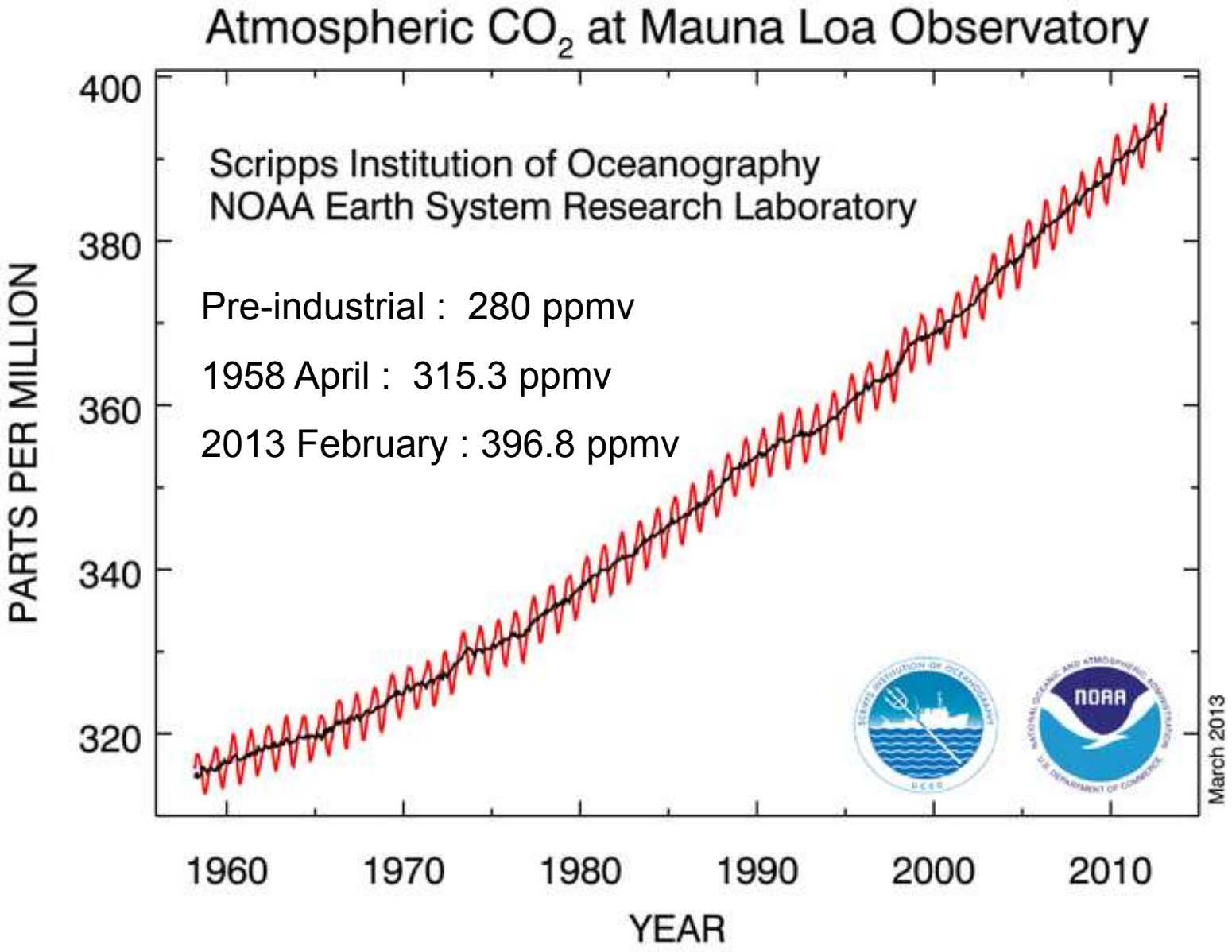

http://www.esrl.noaa.gov/gmd/ccgg/trends/

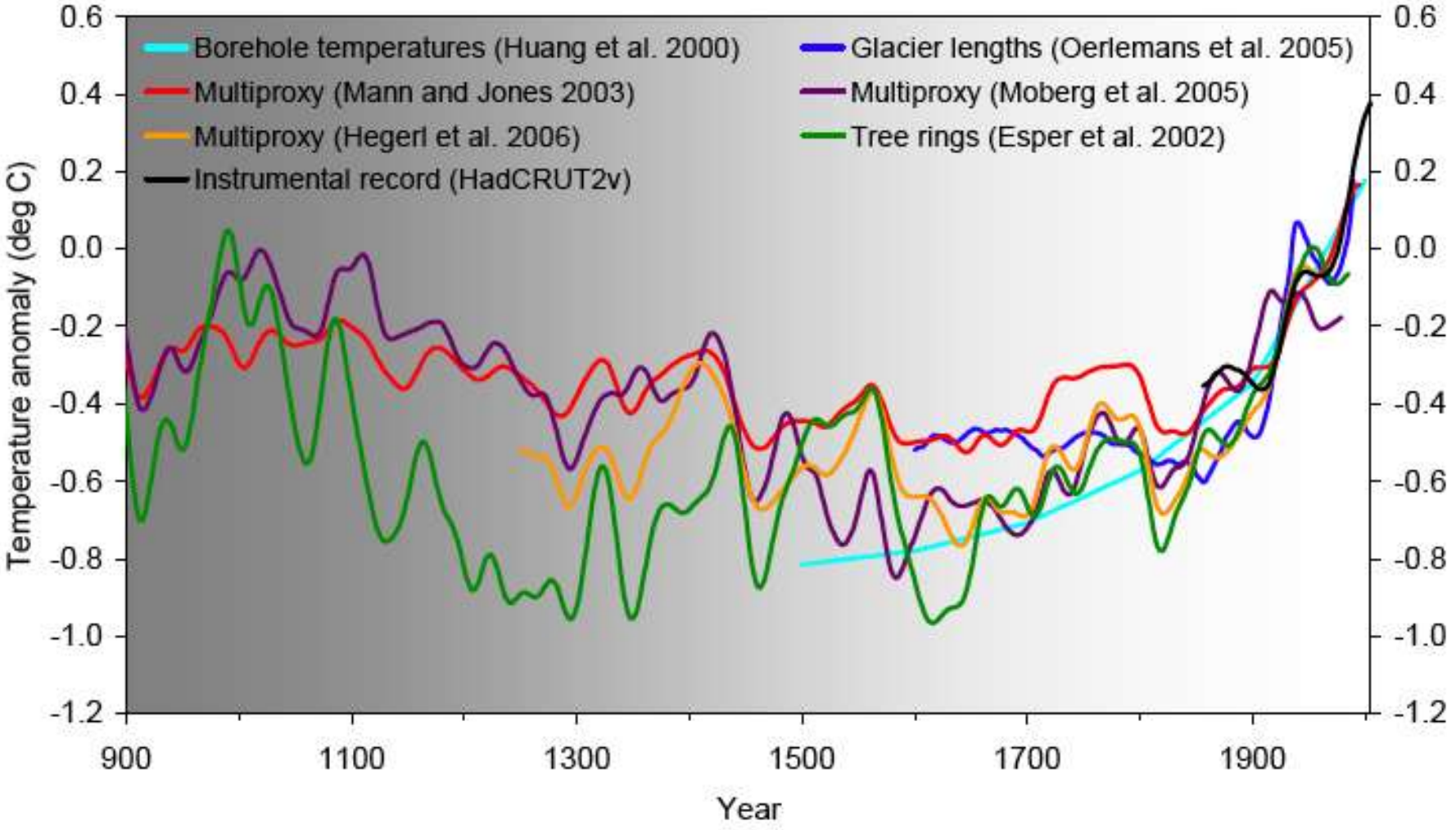
Borehole temperatures (Huang et al. 2000)
Multiproxy (Mann and Jones 2003)
Multiproxy (Hegerl et al. 2006)
Instrumental record (HadCRUT2v)
Glacier lengths (Oerlemans et al. 2005)
Multiproxy (Moberg et al. 2005)
Tree rings (Esper et al. 2002)
Temperature anomaly (deg C)
0.6
0.4
0.2
0.0
-0.2
-0.4
-0.6
-0.8
-1.0
-1.2
900
1100
1300
1500
1700
1900
Year

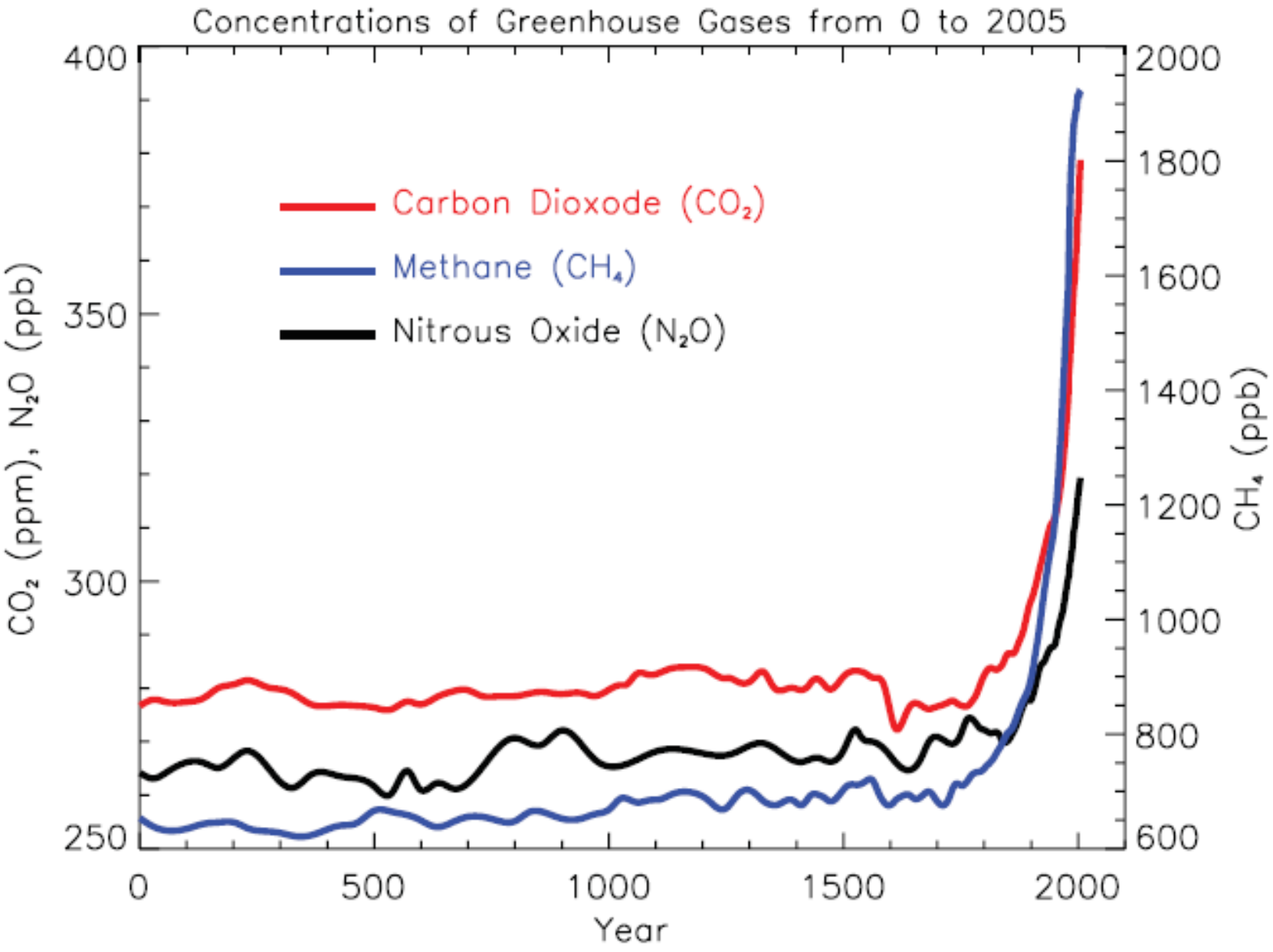
Concentrations of Greenhouse Gases from 0 to 2005
Carbon Dioxode (CO_2)
Methane (CH_4)
Nitrous Oxide (N_2O)
CO_2 (ppm), N_2O (ppb)
CH_4 (ppb)
Year
400
350
300
250
2000
1800
1600
1400
1200
1000
800
600
0
500
1000
1500
2000

Belgian Antarctic Station Princess Elisabeth, Utsteinen Ridge 71 57'S, 23 21'E

Site de EPICA Dome C

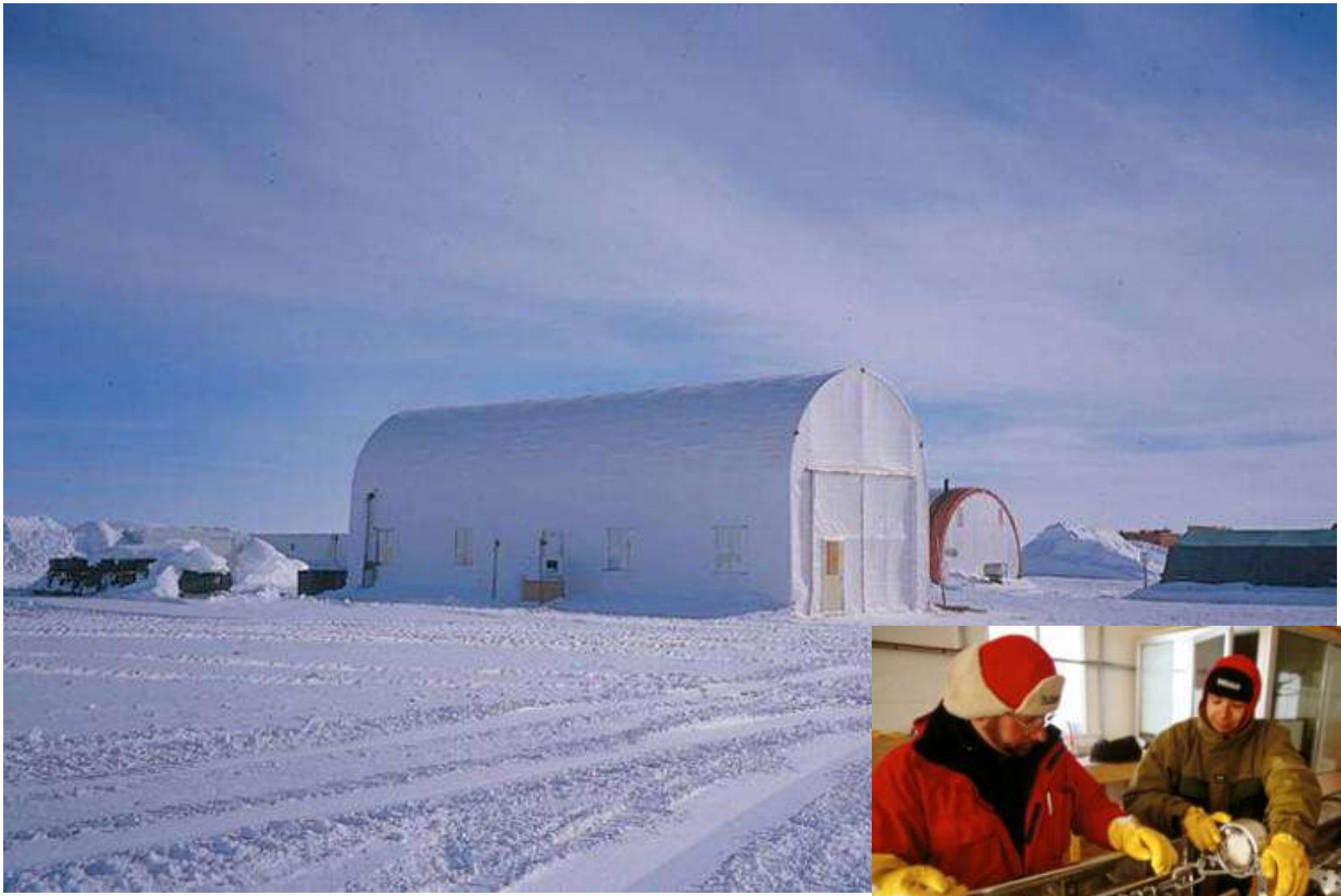

394 in 2012

In 2003 : 465 ppmv CO_{2eq}

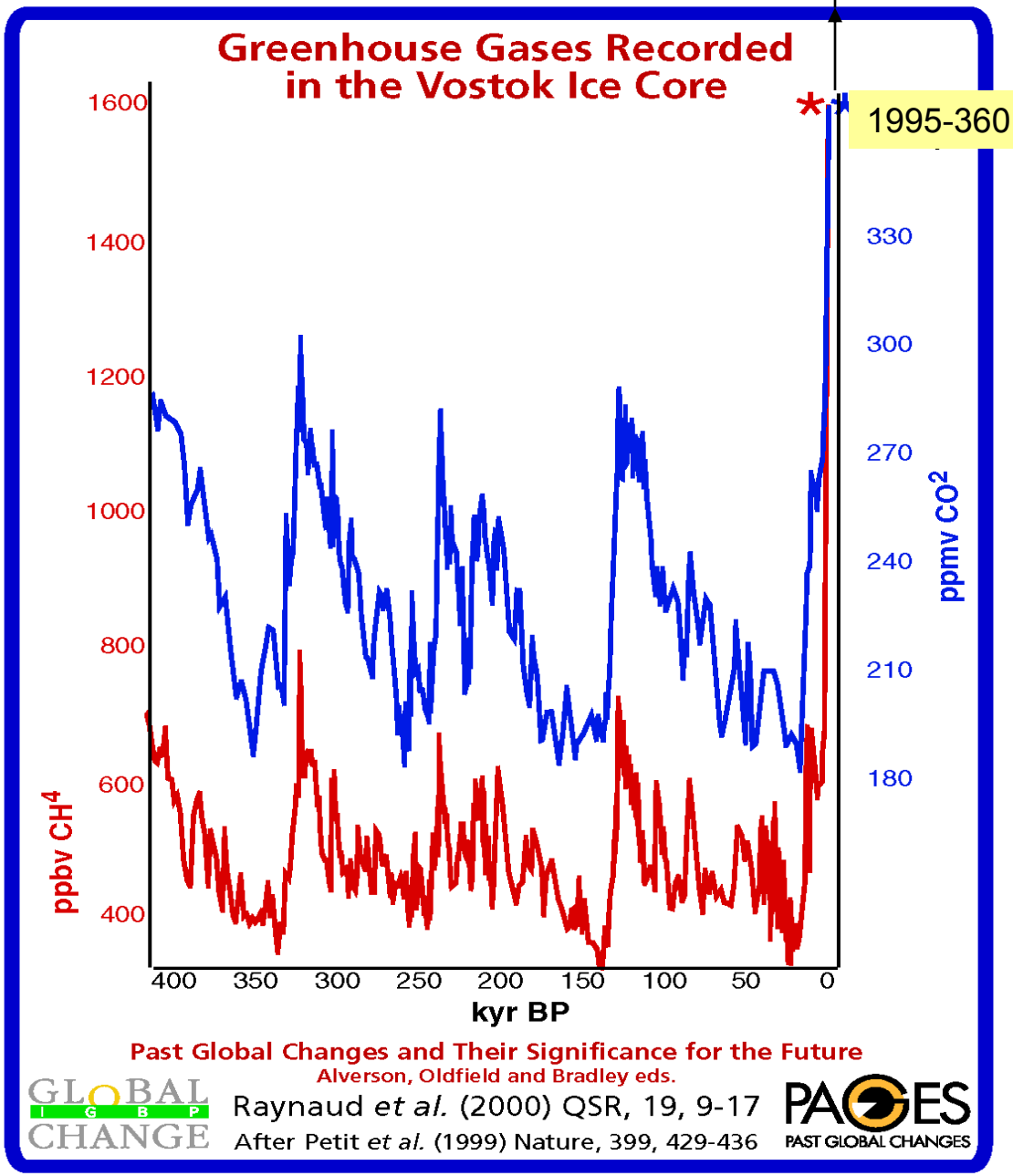

Increase rate

2000-01 : 1.5

2001-02 : 2.0

2002-03 : 2.5

Enregistrements marins

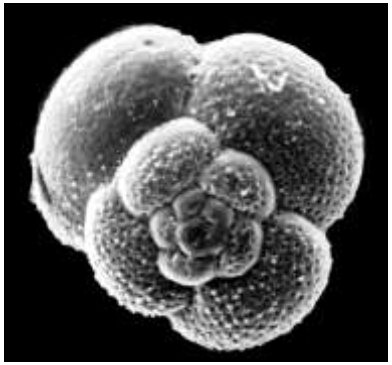

Navire de recherche
« Marion Dufresne »
Institut Polaire Français
IPEV

Franck Delbart / IPEV

Carottier géant du « Marion Dufresne »

Quaternary loess-soil sequences in northern China

S5-1: MIS-13

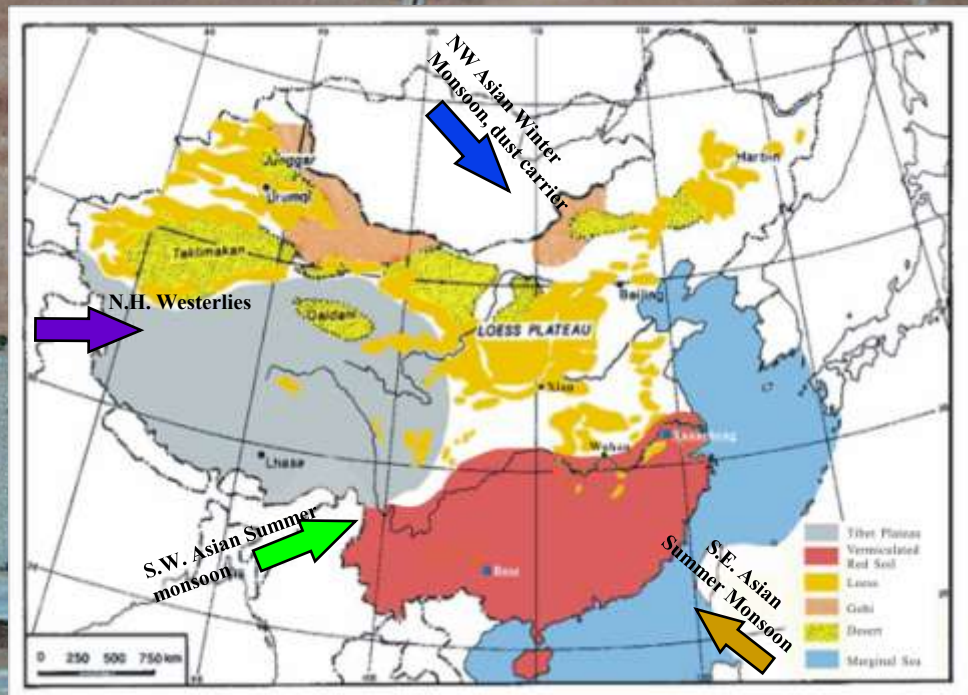

Photo from Institute of Earth Environment, CAS

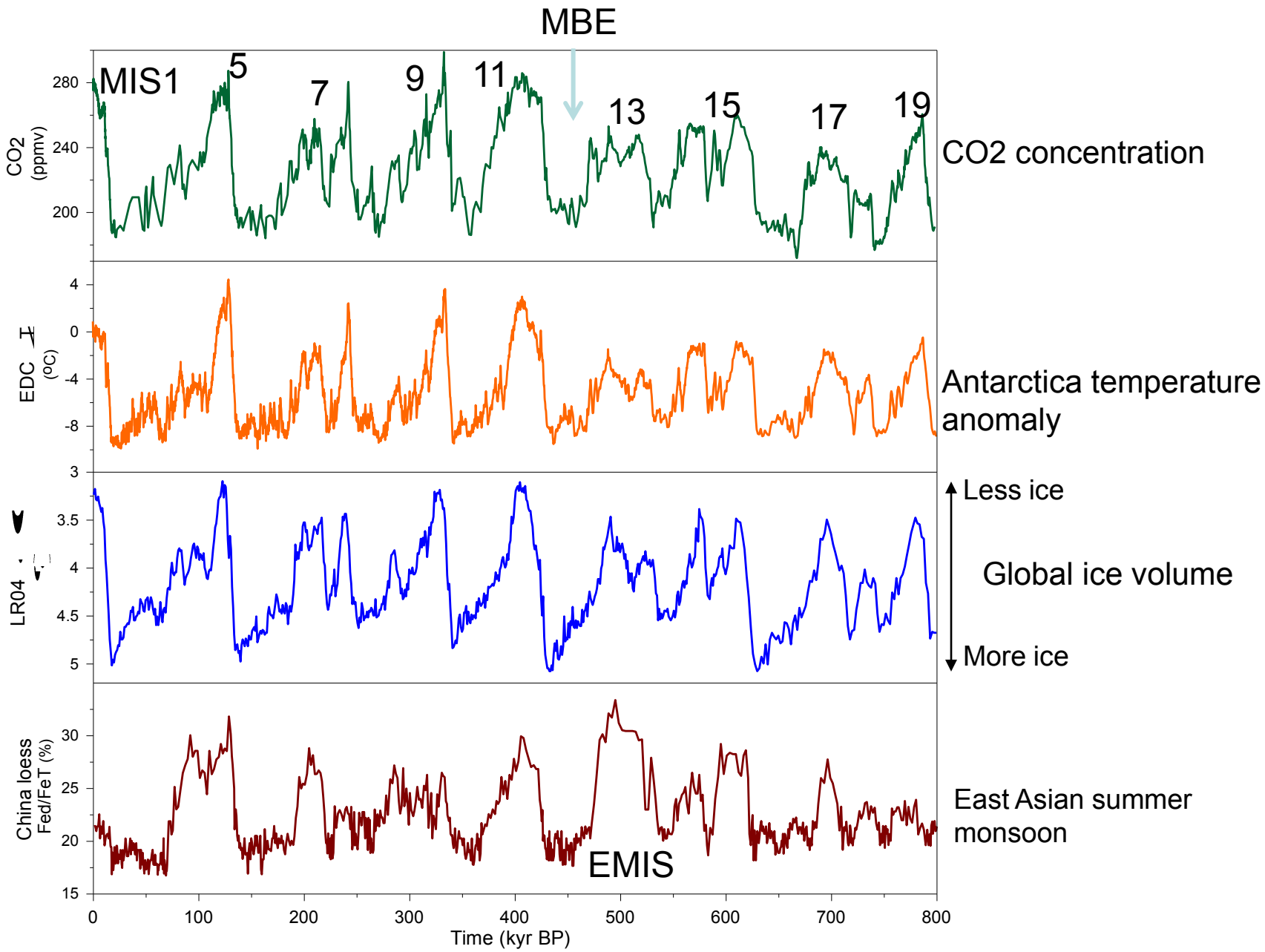

Loulergue et al., 2008; Jouzel et al., 2007; Lisiecki and Raymo, 2005; Guo and Yin, 2009, Yin, 2013

Last Glacial Maximum 21kyr BP

Pre-industrial CO_2 = 280 ppmv

2000 AD CO_2 = 370 ppmv

ΔT=-5 C

Δsea level = –130m

Δice volume = +52 $10^6 km^3$

CO_2 = 200 ppmv

(Joussaume, 1993)

ATMOSPHERIC CO_2 CONCENTRATION

Last Glacial Maximum to Present

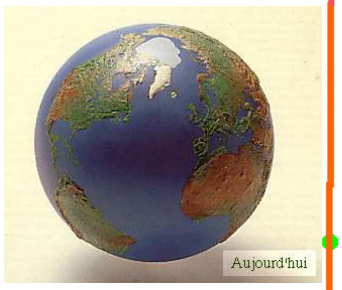

Taylor Dome
Byrd Station
Siple Station
Mauna Loa

CO_2 (ppmv)

360
340
320
300
280
260
240
220
200
180

60000
50000
40000
30000
20000
10000
0

age (yr BP)

Ref. : PAGES and Joussaume,1993

http://www.climate;unibe.ch/gallery_co2.html

CO2eq deviation from the average of the last 9 interglacials

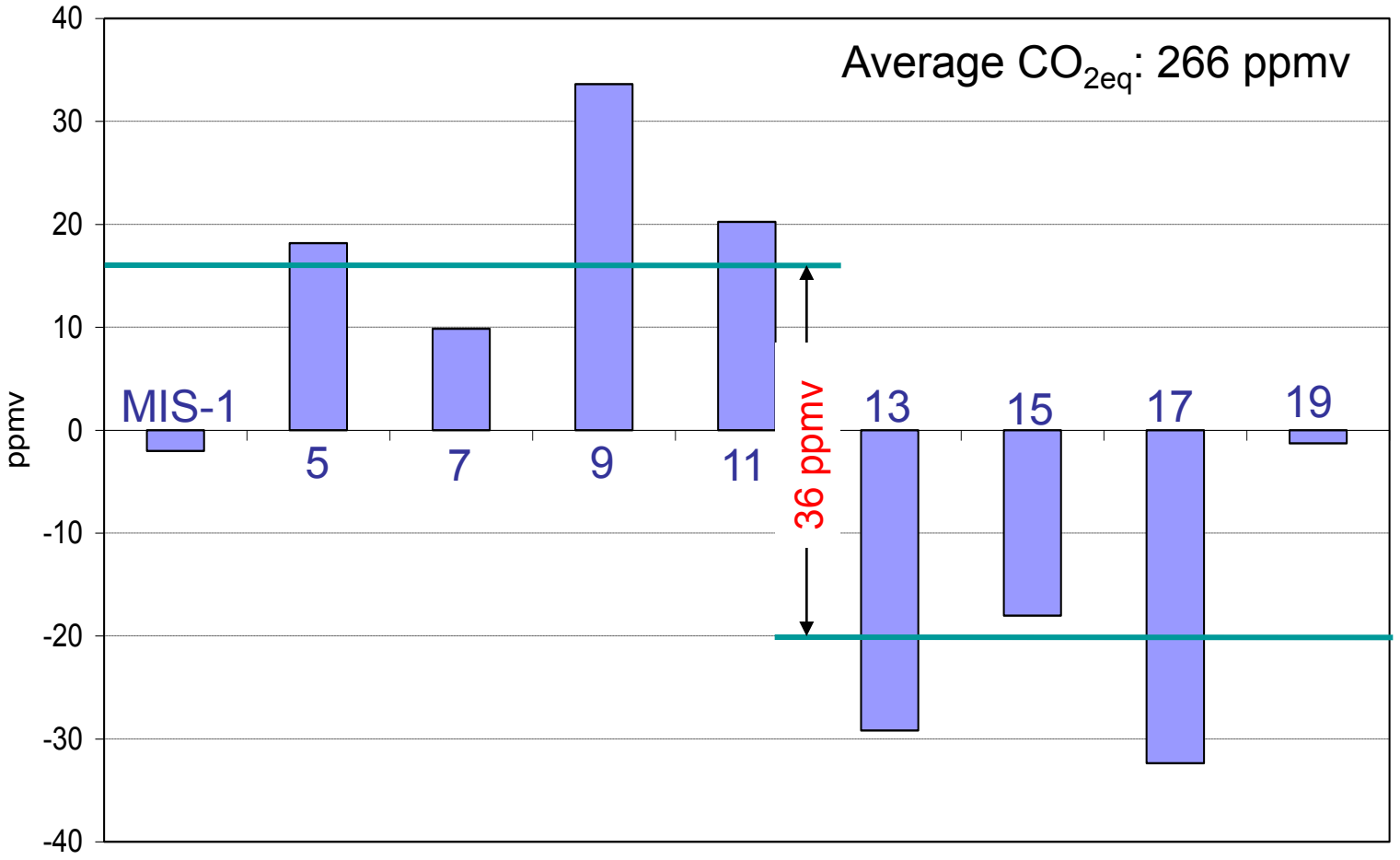

Fig. 5. Insolation at each interglacial minus the insolation calculated from the orbital parameters averaged over the last 9 interglacials e = 0.0328 obl = 23.82

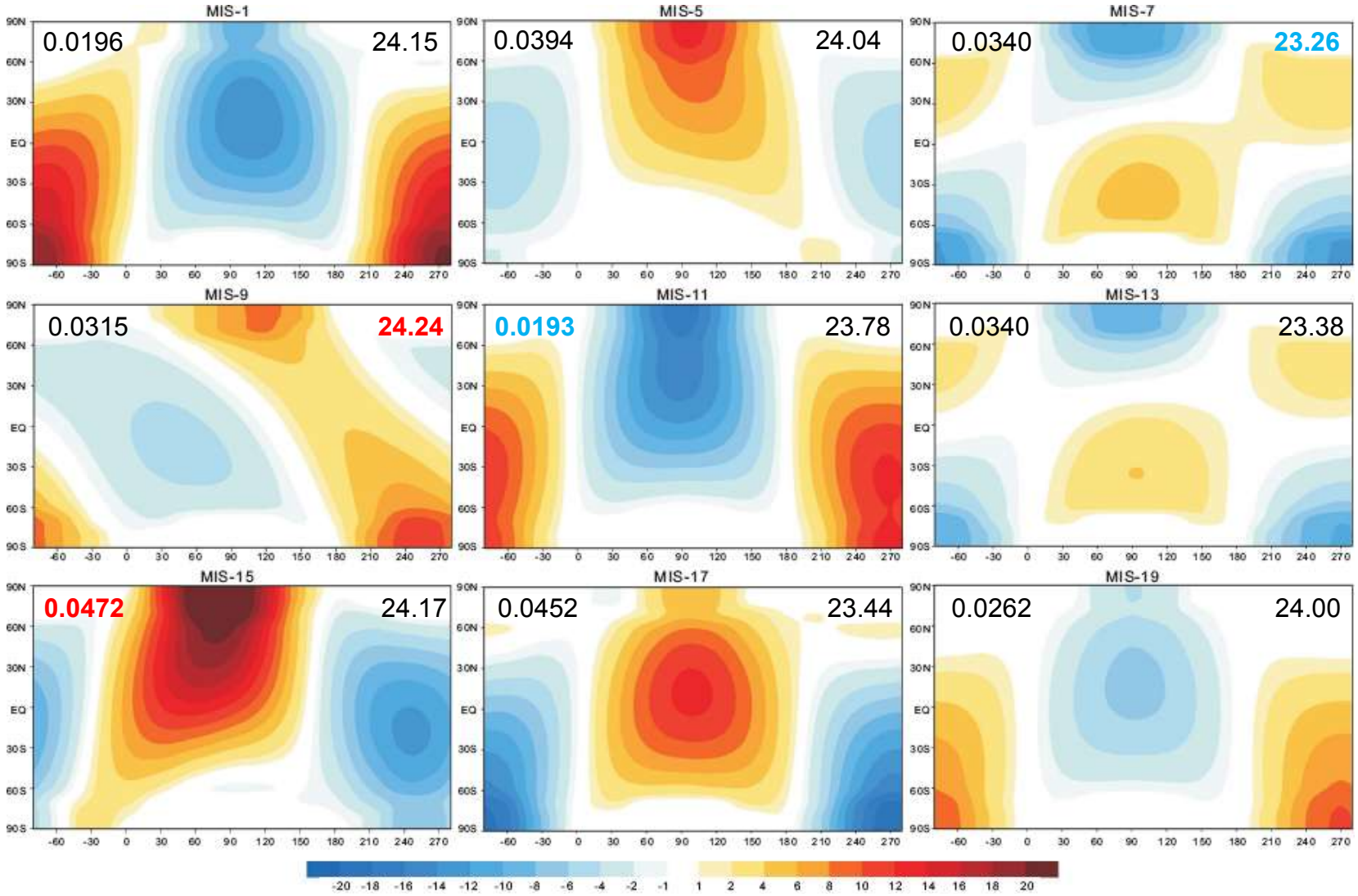

Berger, 1978; Yin and Berger, 2012

Relative importance of GHG and insolation on the warmth intensity is different from one interglacial to another.

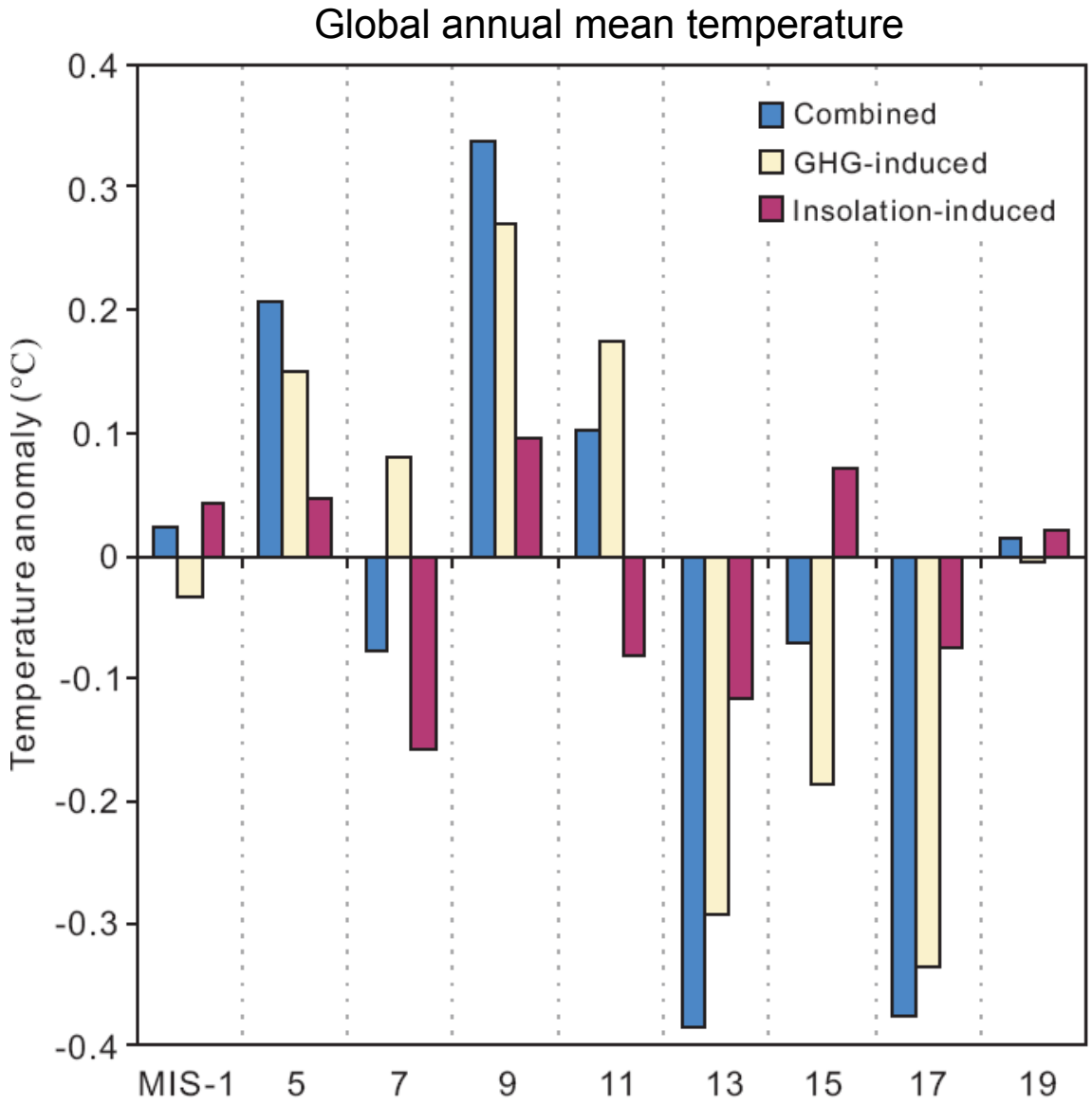

Insolation plays a dominant role on tree fraction, leading to the absence of MBE.

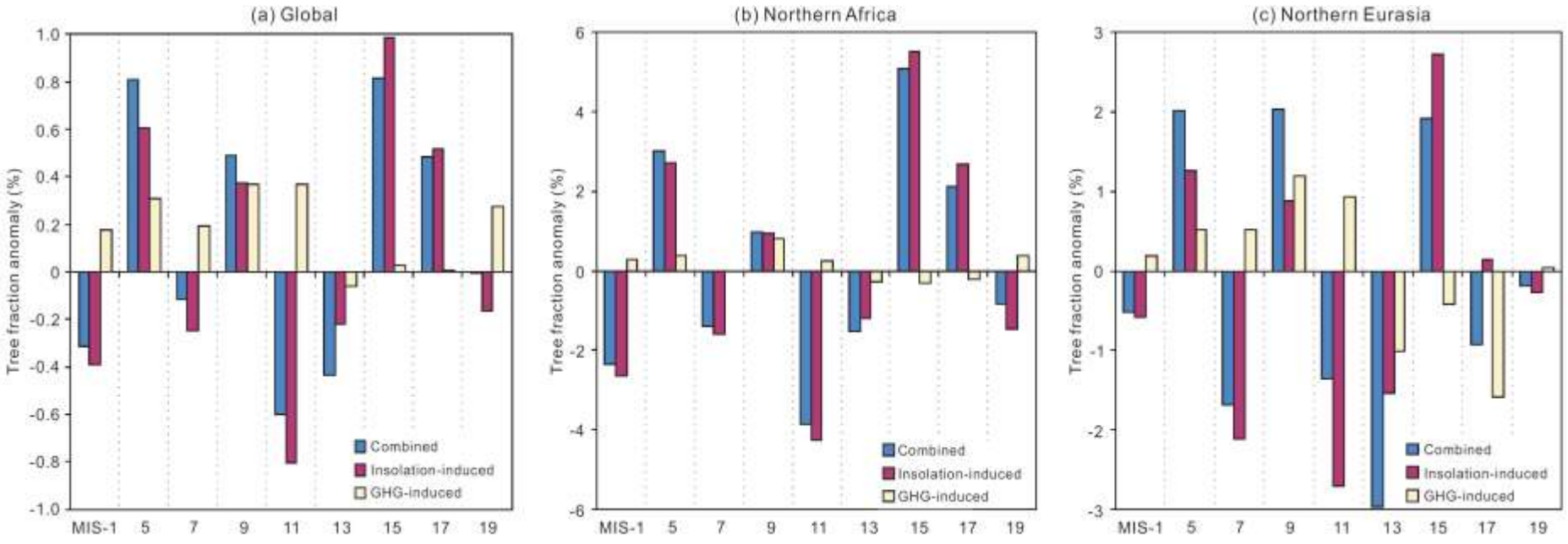

	global	northern Africa	northern Eurasia
GHG-induced	0.26	0.08 *	0.51
Insolation-induced	1.03	1.02	0.92

	global	northern Africa	northern Eurasia
eccentricity	0.96	0.98	0.77
obliquity	0.47	0.41	0.76

CO_2 emissions

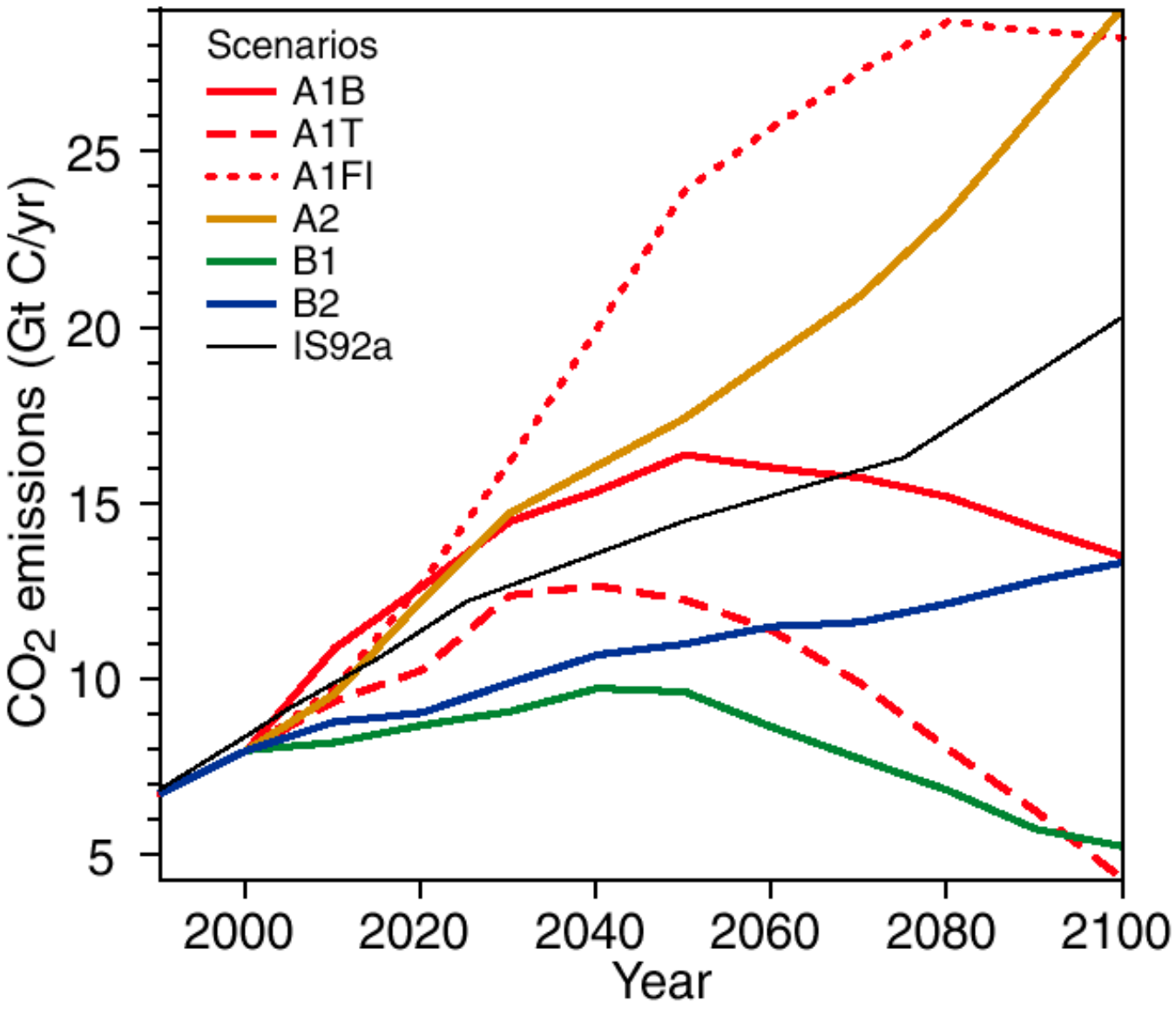

IPCC, 2001

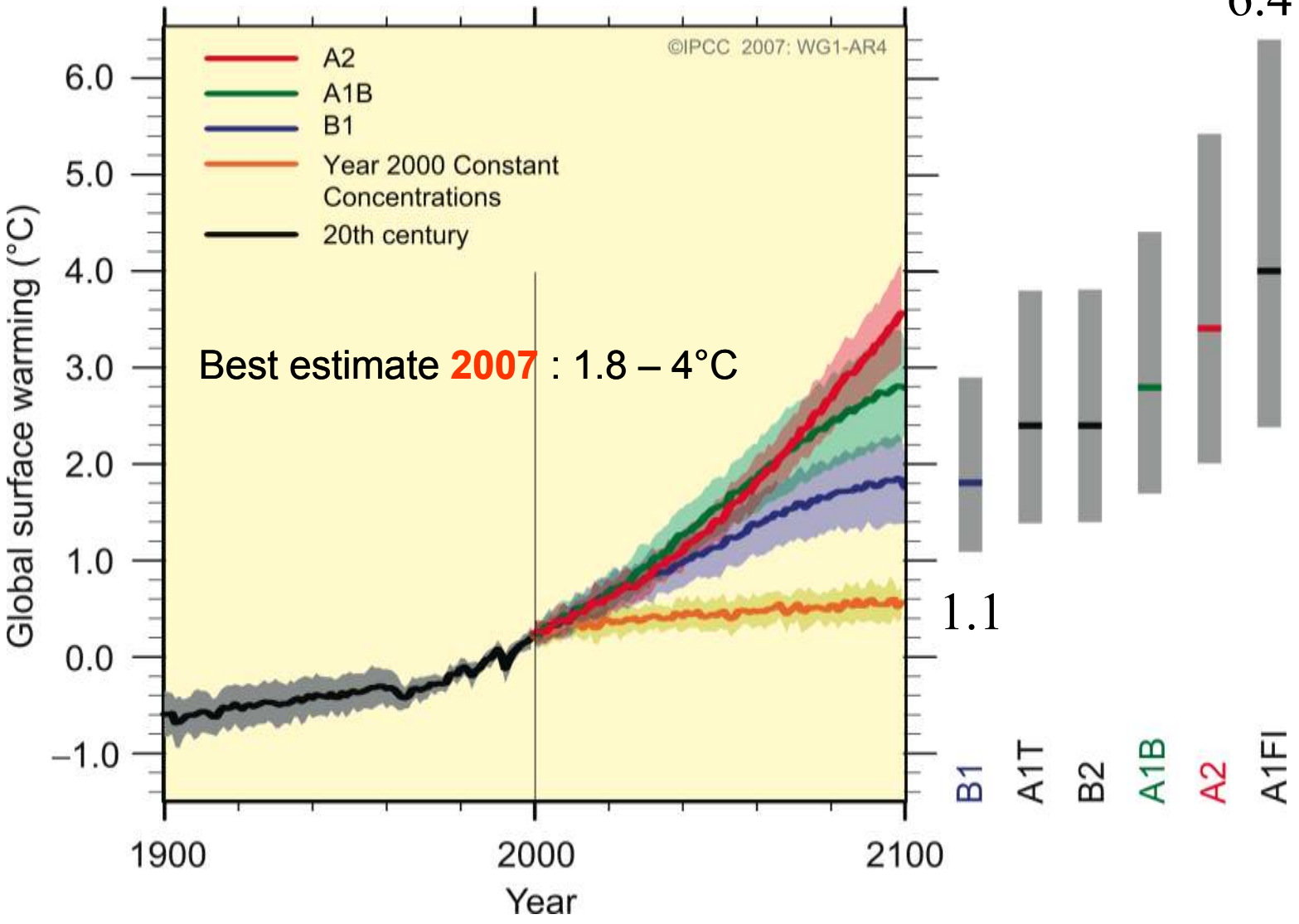

GLOBAL WARMING PREDICTION (IPCC, 2007)

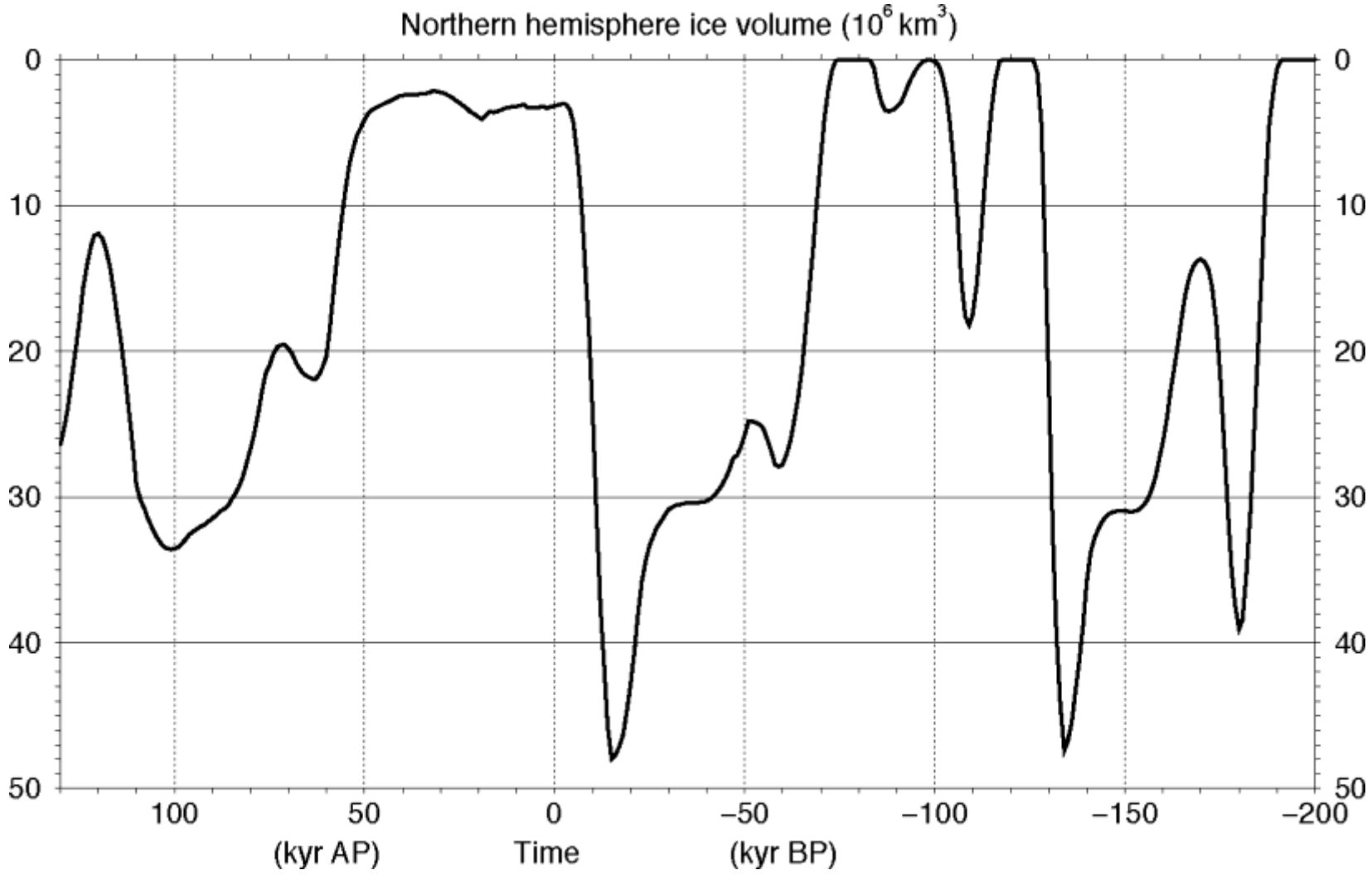

Berger et al., Ambio 1997, Science 2002, Surveys in Geophysics, 2003

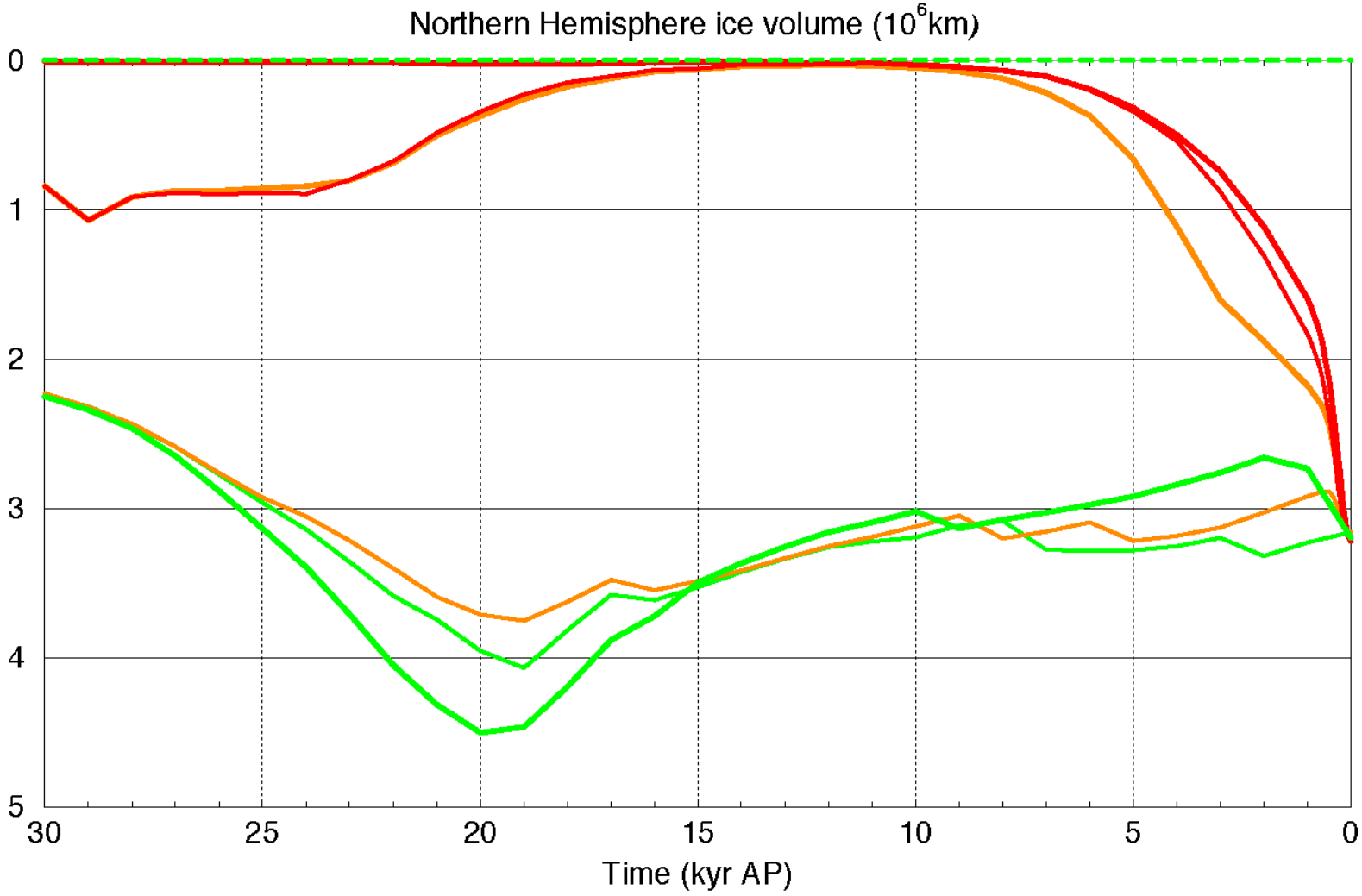

Berger, 2002

Berger and Loutre, 2002

tin line – initial conditions from run –200 – 0

thick line – initial conditions from run –122 – 0

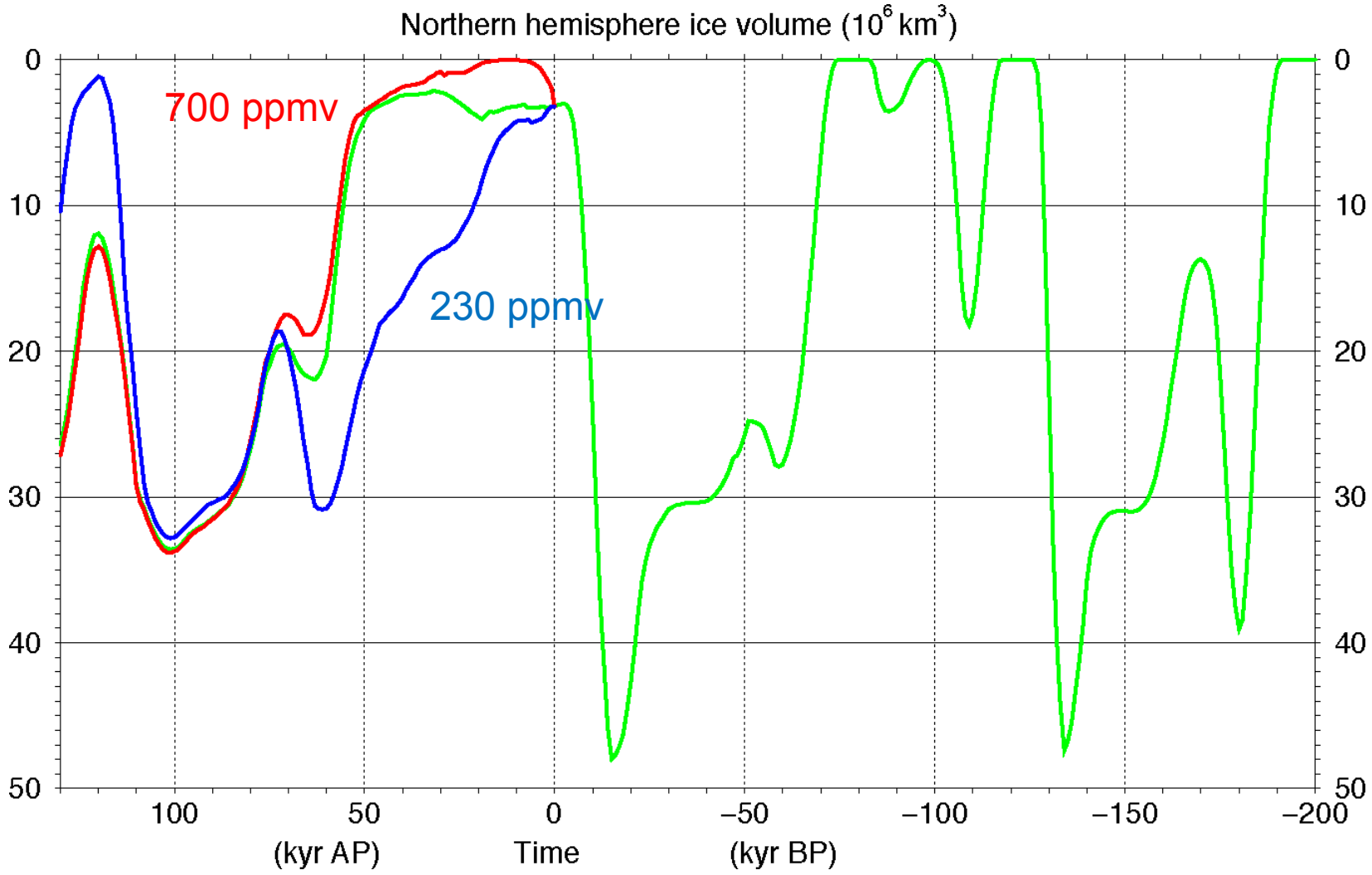

(Berger and Loutre, 2002)


AGIR MAINTENANT POUR
LES GÉNÉRATIONS FUTURES
MAIS RÉFLÉCHIR D'ABORD
MERCI DE VOTRE ATTENTION